

A Cross Iteration Estimator with Base Vector for Estimation of Electric Mining Haul Truck's Mass and Road Grade

Ying Zhang, *Student Member, IEEE*, Yingjie Zhang, Zhaoyang Ai, *Member, IEEE*, Yun Feng and Zuolei Hu

Abstract—Vehicle mass and road grade are important to traction control and safety control of electric mining haul trucks (EMHTs), especially to autonomous EMHTs. This paper proposes a base-vector based cross iteration estimator (BVCIE) to simultaneously estimate the vehicle mass and the road grade for EMHTs. To develop the estimator, the dynamics model for EMHTs is first built and the unknown parameters are identified by the recursive least square (RLS). Then the estimator is proposed by selecting a base vector from the parameters to be estimated, and by using a cross iteration strategy to update older information. This estimator is based on the ideology that the total mass of EMHT is a constant in every travelling trip. The estimator is finally validated on different loads under different road conditions with 930E. The experimental results show that both the vehicle mass and the road grade can be estimated with good accuracy.

Index Terms—Adaptive estimator, electric vehicles, parameter estimation, state estimation, vehicle dynamics identification.

I. INTRODUCTION

THE EMHTs assume an important role in the open-pit mine transportation [1]. As EMHTs are among the most challenging applications of power electronics in the advanced electric vehicle systems, the stability control and the traction control are crucial to safety operation and fuel economy. The EMHTs have a strong hill climbing performance and an

excellent speed controlling performance. They are mostly used where there are uphill grades that may extend several kilometers long [2]. For their crucial role in the mining transportation, the number of EMHTs is also rapidly increasing with the continuous expansion of the open-pit mines in recent years [3-4]. EMHTs take up a great proportion of the coal and iron ore mining transportation in the world, in which the coal mining occupies 40%, and the iron ore 90% respectively [5]. In the operation of mining, more than 50% of mining costs are generally allocated to loading and transportation [6-8], which is a big sum of expense. The latest researches indicate that the EMHT selection [9-10] and control strategies [11-15] have a significant effect on energy consumption and efficiency improvement. The EMHTs are working under extreme mining road conditions [16-17], with many safety problems [18-19]. In order to decrease safety problems and expenditure, increase efficiency and productivity, and extend tyre life and save fuel, the autonomous/semiautonomous EMHTs research becomes a new direction in the recent years [20-21]. The development of EMHTs adds to the urgent demand for reliable technologies to guarantee their safe operation, efficient production and low-cost transportation.

There are many literatures concerning researches of safety control and traction control based on power matching of EMHTs. They indicate that vehicle states and road conditions are important factors affecting EMHTs efficiency, and safety and fuel consumption. According to the latest research, there are many influencing factors such as payload, vehicle speed, mine haul road condition, traffic layout, weather condition and drive skill on the fuel consumption [22]. In traction control, the literatures [12-14] researched the traction control of EMHT, and pointed out that the power matching is an important rule when designing a controller. To abide by the rule of power matching, the required power in the real time needs to be considered when designing the traction system controller. However, the required power is related to vehicle states and road conditions, and the new researches indicate that the EMHT performance is related to mine road conditions and vehicle states [23-24]. Therefore, the vehicle mass and the road grade are important factors to the traction control system. In safety control, the literature [25] indicates that the vehicle mass and the road grade are important to the research on vehicle safety control systems. In the actual operation process, the total mass is different owing to EMHT's highly variable loads,

Manuscript received August 21, 2017; revised September 20, 2017 and December 07, 2017; accepted January 11, 2018. Date of current version January 15, 2018. This work was supported by the National Natural Science Foundation of China (51674113), Natural Science Foundation of Hunan Province (2017JJ4003), Hunan Provincial Innovation Foundation For Postgraduate (CX2017B103). Paper no. TII-17-1895. (#The authors of Ying Zhang, Yingjie Zhang Zhaoyang Ai and Yun Feng contributed to the work equally and should be regarded as co-first authors. Corresponding authors: Ying Zhang, Yingjie Zhang and Zhaoyang Ai. *To whom correspondence should be addressed: zhangying14@hnu.edu.cn; zhangyj@hnu.edu.cn; aizhaoyang@hnu.edu.cn.)

Ying Zhang, Yingjie Zhang and Zuolei Hu are with the College of Computer Science and Electronic Engineering, Hunan University, Changsha, 410082, China. (e-mail: zhangying14@hnu.edu.cn; zhangyj@hnu.edu.cn; huzuolei@hnu.edu.cn).

Zhaoyang Ai is with the Institute of Cognitive Control and Lingua-biolinguistics, CFL, Hunan University, Changsha, 410082, China. (aizhaoyang@hnu.edu.cn).

Yun Feng is the Company of Bozhon (Suzhou) Precision Industry Technology Co., Ltd, Jiangsu province, Suzhou, 215217, China. (e-mail: 13142034527@163.cn).

Color versions of one or more of the figures in this paper are available online at <http://ieeexplore.ieee.org>.

which is often susceptible to a large change from load to unload. At the same time, the road grade varies with different mine road conditions. As the simultaneous estimation of the vehicle mass and road grade in the real time is a difficult problem, the extensive control methods do not consider the variation when the controller is designed [26-28].

The methods for estimating vehicle mass and road grade are widely studied in the past few years in solving the problems of traction control, vehicle safety, power delivery, fuel savings, *et al.* [29-31]. The studies in the literature [32] applied the sensor-based method to obtaining the time-varying nature of the road grade; then a conventional parameter estimation method is used for the estimation of vehicle mass [33]. This, however, may lead to sophisticated hardware and high complexity. At the same time, the accuracy is easily affected by disturbances of sensors [34]. The literature [35] used Global Positioning System (GPS) for the estimation of road grade and vehicle parameter, but this method does not completely work well in case of shelter conditions. Moreover, the cost of this method is higher.

Compared with the sensor-based method, the model-based estimation method has a better performance because the measurement is not required. In the latest researches, the estimation of the vehicle mass, road grade and other vehicle parameters and states by model-based methods are extensively focused [36-41]. The extended Kalman filter (EKF) for the estimation of road grade and vehicle mass on line is proposed in [42], and the simulated results show a good performance. But the unconstrained Kalman filter finds difficulty in guaranteeing convergence to address a constrained state estimation problem in physical systems. To overcome this defect, a constrained dual Kalman filter based on probability density function (pdf) truncation method is proposed to solve the constrained state estimation problem [43]. The traditional RLS estimation method is quite straightforward in estimating the vehicle parameters, and the tested results show a good performance [44-45]. But the test results in [46] show that the traditional RLS is not good when estimating the vehicle state. Moreover, the RLS with single forgetting factor is not good, either, owing to the varying state vectors on the same rate, which can easily result in convergence when the road grade is constantly changing [47]. To address this problem, the RLS method with multiple forgetting factors is proposed in [46-48], but the non-optimal selections of the forgetting factors will lead to low accuracy of their estimation results or even big errors. To improve the accuracy, a hybrid algorithm combining EKF and RLS is proposed in [49-50], and a hybrid algorithm combining EKF and Luenberger Observer (LO) is proposed in [31]

respectively to estimate vehicle mass and road grade. Although the hybrid algorithms are better than the single algorithms, it will lead to high complexity.

In this paper, a new BVCIE for simultaneous estimation of vehicle mass and road grade is proposed, and is applied to EMTHs in estimating its total mass and road grade on line. The estimation method proposed in this paper takes advantage of the fact that the total mass is a constant during every travelling trip. With this in mind, we select the total mass as a base vector. Then, according to the relationship in the vehicle longitudinal dynamics model, the cross iteration strategy for the discarding of older information in favor of newer information is proposed, and the convergence of the cross iteration strategy is proved.

This paper is organized as follows. In Section II, a longitudinal dynamics model of EMHT is described, and the unknown parameters are identified with recursive least square. In Section III, the algorithm of BVCIE is proposed with proof. In this section, the method of the estimating road grade and vehicle mass using BVCIE is presented. In Section IV, the estimator performance is verified with real operation data to estimate road grade and vehicle mass, and the results are analyzed in detail. Finally, the conclusion is given in Section V.

II. VEHICLE DYNAMICS AND PROBLEM FORMULATION

In this section, The EMHT's model will first be given. Then, the unknown parameters, effective rolling friction coefficient μ and air resistance coefficient C_d will be identified by recursive least square method and the EMHT model will be verified with a 930E. Finally, it is followed by the problem statement.

A. Longitudinal Dynamics

The analysis of the EMHT's force in its running on the mine haul road is shown in Fig. 1. To simplify the exposition of the EMHT's longitudinal dynamics model, the following assumptions are made:

Assumption 1: For a realistic road condition, the road grade is continuous with respect to the longitudinal position, given that the EMHT's longitudinal velocity is also a continuous function of time.

Assumption 2: Road grade is assumed to be the varying function of time, whereas the EMHT's mass is assumed to be an unknown constant.

Assumption 3: In the EMHT's traveling process, it is assumed that the brake is not working at any times. Thus, the friction brakes are never applied. To detect whether the brake is applied, the system controller just needs to detect whether the brake paddle is in the idle state.

Assumption 4: In the traveling process, the values of effective

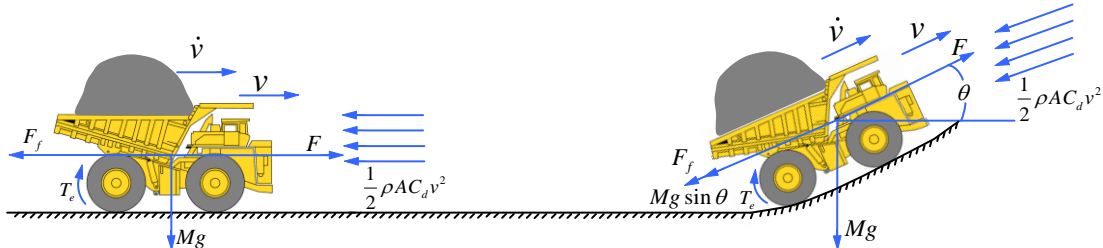


Fig. 1. Longitudinal forces acting on the EMHT on the mining road.

rolling resistance coefficient and air resistance coefficient are unknown constants in the same environmental condition. Therefore, these parameters need to be identified before vehicle mass and road grade are estimated.

Assumption 5: In the traveling process, the effect of shaking force is not considered.

Assumption 6: In the traveling process, the air/wind resistance is not considered due to the air/wind speed and its uncertainty of incident angles, and the wind resistance is very small compared with other forces.

Assumption 7: In the traveling process, the transmission gear resistance is not considered because the loss caused by transmission gears is very small.

As shown in Fig. 1, according to Newton's Second Law in the longitudinal dynamics and the above assumptions, the nonlinear vehicle longitudinal dynamics can be expressed as follows:

$$F = F_w + F_f + F_i + M\dot{v} \quad (1)$$

where F is EMHT's driving force, F_f , F_w , F_i refer to air resistance, rolling resistance and ramp resistance, respectively. M is the total mass of EMHT. \dot{v} is acceleration of EMHT's longitudinal velocity. The driving force F is from traction motors embedded in the two rear wheels of EMHT. For traction motors, the total torque T_e can be obtained by monitoring motor's current and flux by using sensors. If the wheel radius is r , the EMHT's driving force can be expressed as follows:

$$F = \frac{T_e}{r} \quad (2)$$

The air resistance F_f is related to air density ρ , drag coefficient C_d , forward velocity v and frontal area A of EMHT, which can be expressed as follows:

$$F_f = \frac{1}{2} \rho A C_d v^2 \quad (3)$$

The rolling resistance F_w is determined by road conditions and total vehicle mass, which can be expressed as follows:

$$F_w = Mg \mu \cos \theta \quad (4)$$

where μ is the effective rolling friction coefficient, θ is the road grade, g is the acceleration due to gravity. The ramp resistance is caused by road grade, which can be expressed as follows:

$$F_i = Mg \sin \theta \quad (5)$$

Substituting (2), (3), (4) and (5) into (1), the longitudinal dynamics can be written as:

$$\dot{v} = \frac{2T_e}{Mr} - \frac{1}{2M} \rho A C_d v^2 - \mu g \cos \theta - g \sin \theta \quad (6)$$

B. Parameters Identification and Model Validation

For the model in Section II(A), the parameters of effective rolling friction coefficient μ and drag coefficient C_d are not constants in different mining scenarios. Therefore, it is required to identify these parameters for a specific mining scenario. However, the real values of the effective rolling friction coefficient μ and drag coefficient C_d are difficult to be obtained directly from the measurements by on-board sensors or other devices. To make equation (6) in II(A) a practical model and usable in estimating vehicle mass and road grade, the parameters of the effective rolling friction coefficient μ and the drag coefficient C_d need to be identified in priori by some real running data and vehicle parameters, including wheel radius,

air density, vehicle frontal area, vehicle total mass, acceleration due to gravity, vehicle velocity and acceleration, motors torques and road grade. The following RLS method is used to solve this problem.

In an effort to further develop an identification strategy, the dynamics model from (6) can be written as follows:

$$y = H\alpha + U \quad (7)$$

where $y = \dot{v}$, $U = 2T_e / (Mr)$, $H = [H_1, H_2] \in \mathbb{R}^{1 \times 2}$, H_1 and H_2 given by

$$\begin{cases} H_1 = -\frac{\rho A v^2(k)}{2M} \\ H_2 = -g \end{cases} \quad (8)$$

In (8), $\alpha = [\alpha_1, \alpha_2] \in \mathbb{R}^{2 \times 1}$, which can be written as follows:

$$\begin{cases} \alpha_1 = C_d \\ \alpha_2 = \mu \end{cases} \quad (9)$$

The RLS method is selected so that it minimizes loss function as follows:

$$J(\alpha, k) = \frac{1}{2} \sum_{i=1}^k (y(i) - H(i)\alpha(i) - U(i))^2 \quad (10)$$

The RLS method is introduced to discard older information in favor of newer information. The recursive solution can be expressed as follows:

$$\hat{\alpha}(k) = \hat{\alpha}(k-1) + K(k)(y(k) - H(k)\hat{\alpha}(k-1)) \quad (11)$$

where

$$K(k) = P(k-1)H(k)(H(k)P(k-1)H^T(k) + 1)^{-1}$$

and

$$P(k) = (I - K(k-1)H(k))P(k-1)$$

To prove that the RLS can identify the effective rolling friction coefficient μ and drag coefficient C_d , and can satisfy the PE condition, a detailed analysis is given as follows.

The linear system can be expressed as follows:

$$Y = H\alpha \quad (12)$$

where $Y = \dot{v} - 2T_e / (Mr)$. According to [51], for any $k > 0$, when there exist $t > 0$, and $\sigma_1 > 0$, $\sigma_2 > 0$, and equation (13) is true, then the RLS satisfies the PE condition.

$$\sigma_1 I \leq \sum_{i=k}^{k+t} HH^T \leq \sigma_2 I \quad (13)$$

According to (12), the HH^T can be expressed as follows:

$$HH^T = [H_1, H_2] \times \begin{bmatrix} H_1 \\ H_2 \end{bmatrix} = \frac{\rho^2 A^2 v^4}{4M^2} + g^2 \quad (14)$$

As v belongs to bounded vector, and ρ , A , g , M belong to different fixed parameters, it is obvious that equation (14) satisfies equation (13). Therefore, the RLS that identifies the effective rolling friction coefficient μ and the drag coefficient C_d satisfies the PE condition in theory. Moreover, to guarantee that the signals in real experiments are persistently exciting, the signals need to be completely synchronized so as to be collected.

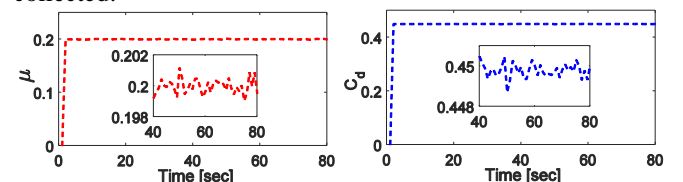


Fig. 2. Identification results of effective rolling friction coefficient μ and drag coefficient C_d .

The experimental data used to identify the parameters of effective rolling friction coefficient μ and drag coefficient C_d are obtained by the 930E, a general kind of EMHT produced by Komatsu. According to the RLS estimator (11), to identify the parameters of the effective rolling friction coefficient μ and the drag coefficient C_d , the road grade needs to be known by priori. For this problem, we select a bumpy test road with approximately 560 meters, and the total mass is approximately $M=260000$ kilograms. The road grade is calculated by the relative height of road information which is obtained by GPS assisted by fixed and mobile base stations. By the method of RLS, the parameters of effective rolling friction coefficient μ and drag coefficient C_d can be obtained and the results are shown in Fig. 2. As shown in Fig. 2, it can be known that the parameters estimated by RLS have a fast and robust convergence. According to the part of enlarged curves in Fig. 2, the estimated values were expected to vary during the test. But the variations are very small, so we take the average value $\hat{\mu}=0.2$ and $\hat{C}_d=0.45$ as the estimated value. In order to guarantee the rationality of the model, the identified μ and C_d need be verified when used for the estimation of vehicle mass and road grade. For this problem, we verified parameters μ and C_d and the model with the real running velocity of the same 930E, but the test selected another bumpy test road with about 2100 meters in distance. With this method, we can simultaneously verify the estimated parameters and the built model, and this method has been successfully used in literature [41]. The validation result is shown in Fig. 3.

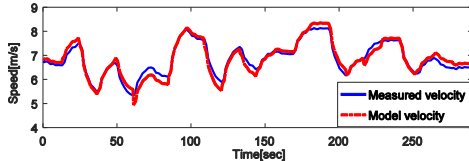


Fig. 3. Results of verifying 930E's model and parameters μ and C_d .

It can be seen from the result in Fig. 3 that there are some deviations between the true and the estimated values, which is because the real system has some disturbances such as the bumpy road condition and the disturbance of sensors. But in general, the model results are close to the actual results, which show that the identified parameters μ and C_d are reasonable.

C. Problem Formulation

The total vehicle mass and road grade are crucial parameters for the EMTH's traction system controller design and the safety system controller design, as shown in Fig. 4. It is obvious that the road grade is a varying function of time, but the total mass of EMHT is a constant. However, the loading capacity of EMHT is not the same in different trips, which leads to the total mass variations in different trips. Therefore, the simultaneous obtaining of the vehicle total mass and the road grade on line is a difficult problem. It should be pointed out that the RLS algorithm possesses many advantages in vehicle parameters estimation. Moreover, based on the results in Fig. 2, it is clear that the method of RLS has a good performance in the estimating of the model's unknown constant parameters in model (6). But, in EMHT's traveling process, the road grade is changed randomly, namely, $\dot{\theta} \neq 0$. Under this circumstance, the RLS estimation strategy is difficult to simultaneously estimate the EMHT's mass and the road grade on line. To

address this problem, the next section will present a BVCIE to simultaneously estimate EMHT mass and road grade.

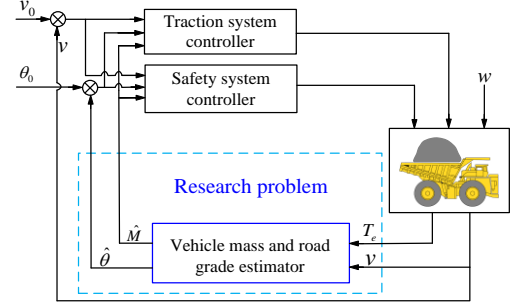


Fig. 4. Structure of the control system with simultaneous estimation of vehicle mass and road grade on line.

III. BVCIE DESIGN

In this section, a new estimator is first proposed. Then, a cross iteration law is proposed and its convergence with detailed analysis and proof is presented. According to the fact that the total vehicle mass is a constant during every trip, the iteration law with base vector is finally proposed and is proved in detail.

A. Estimator Design

In order to further develop the estimator, we can rewrite the equation (6) with the following linear form:

$$y = \phi x \quad (15)$$

where $y = \dot{v}$, $\phi = [\phi_1, \phi_2] \in \mathbb{R}^{1 \times 2}$, ϕ_1 and ϕ_2 obtained from

$$\begin{cases} \phi_1 = \frac{2T_e}{r} - \frac{1}{2} \rho A C_d v^2 \\ \phi_2 = -g \sqrt{1 + \mu^2} \end{cases} \quad (16).$$

In (15), $x = [x_1, x_2]^T \in \mathbb{R}^{2 \times 1}$, which can be written as follows:

$$\begin{cases} x_1 = \frac{1}{M} \\ x_2 = \sin(\theta + \theta_\mu) \end{cases} \quad (17)$$

where θ_μ is defined by $\tan(\theta_\mu) = \mu$.

Assuming the vectors of x can be estimated with $\hat{x}(k/k-1)$, where k and $k-1$ are the indexes of the discrete sampling instants, and $\hat{x}(k/k-1)$ represents the estimated vectors of $x(k)$ based on a cross iteration law with base vector. We can easily obtain the system's estimated output according to (15) and it can be expressed as follows:

$$\hat{y}(k) = \phi(k) \hat{x}(k/k-1) \quad (18)$$

where $\hat{x}(k/k-1)$ represents the estimated vectors by a cross iteration law with base vector, and \hat{y} is the estimated output. Based on (15) and (18), we can design the estimator with the following formulation:

$$\hat{x}(k) = \hat{x}(k/k-1) + \phi^{-1}(k)(y(k) - \hat{y}(k)) \quad (19)$$

B. Cross iteration Law

To achieve the estimator (19), the cross iteration law is introduced and can be expressed as follows:

$$\begin{cases} \hat{x}_1(k/k-1) = f_1(k) + g_1(k) \hat{x}_2(k/k-1) \\ \hat{x}_2(k/k-1) = f_2(k) + g_2(k) \hat{x}_1(k-1/k-2) \end{cases} \quad (20)$$

where

$$\begin{aligned} f_1(k) &= \frac{\dot{v}(k)}{\frac{2T_e(k)}{r} - \frac{1}{2}\rho AC_d v^2(k)} & g_1(k) &= \frac{g\sqrt{1+\mu^2}}{\frac{2T_e(k)}{r} - \frac{1}{2}\rho AC_d v^2(k)} \\ f_2(k) &= -\frac{\dot{v}(k)}{g\sqrt{1+\mu^2}} & g_2(k) &= -\frac{\frac{2T_e(k)}{r} - \frac{1}{2}\rho AC_d v^2(k)}{g\sqrt{1+\mu^2}}. \end{aligned}$$

From (20), it is clear that f_1, g_1, f_2, g_2 can be measured with sensors in real time. To prove the convergence of the cross iteration law, a detailed analysis is given as follows.

Theorem 3.1: For the cross iteration law in (20), the vector $\hat{x}_1(k+1/k)$ can be rewritten as follows:

$$\hat{x}_1(k+1/k) = g_1(k+1)x_2(k+1/k) + f_1(k+1) \quad (21)$$

The convergence condition of vector $\hat{x}(k+1/k)$ is: when $k \rightarrow \infty$, there will be $\lim_{k \rightarrow \infty} (\hat{x}_1(k+1/k) - \hat{x}_1(k/k-1)) \rightarrow 0$.

Proof 3.1: According to the cross iteration law in (20), the vector $\hat{x}_2(k+1/k)$ is determined by $\hat{x}_1(k+1/k)$. Thus, to prove the convergence of the cross iteration law (20), it only needs to prove the convergence of $\hat{x}_1(k+1/k)$. When $k \rightarrow \infty$, the vector of $\hat{x}_1(k+1/k)$ can be written as:

$$\begin{aligned} \hat{x}_1(k+1/k) &= f_1(k+1) + g_1(k+1)\hat{x}_2(k+1/k) \\ &= f_1(k+1) + g_1(k+1)f_2(k+1) \\ &\quad + g_1(k+1)g_2(k+1)\hat{x}_1(k/k-1) \end{aligned} \quad (22)$$

According to equation (22), the following relationship can be obtained:

$$\begin{aligned} \lim_{k \rightarrow \infty} (\hat{x}_1(k+1/k) - \hat{x}_1(k/k-1)) \\ = \lim_{k \rightarrow \infty} (f_1(k) + g_1(k)f_2(k)) = 0 \end{aligned} \quad (23)$$

From the above proof, it is obvious that the cross iteration estimator is convergent.

C. Iteration Law with Base Vector

Though the vectors can be converged through iteration calculation, to the cross iteration estimator in (19), it is still difficult to obtain the right solution because the road grade may be different at any two iteration calculations. So in every iteration calculation, there are many solutions for (19). To address this problem, an iteration law with base vector is proposed. In the EMHT's traveling process, the total mass M can be considered as a constant, so the estimated vector of $\hat{x}_1(k/k-1)$ can be selected as a base vector, and in the iteration calculation process, the base vector meets the following law:

$$\hat{x}_1(k+1/k) = \hat{x}_1(k/k-1) \quad (24)$$

By the law of (24), it can obtain the following relationship:

$$\begin{aligned} f_1(k+1) + g_1(k+1)\hat{x}_2(k+1/k) \\ = f_1(k) + g_1(k)\hat{x}_2(k/k-1) \end{aligned} \quad (25)$$

From the relationship in (25), it can obtain a new method to update the vector $\hat{x}_2(k+1/k)$, which can be expressed as follows

$$\hat{x}_2(k+1/k) = \frac{g_1(k)\hat{x}_2(k/k-1)}{g_1(k+1)} + \frac{(f_1(k) - f_1(k+1))}{g_1(k+1)} \quad (26)$$

To verify the convergence of the estimator with cross iteration law and base vector, the following will present a detailed analysis and proof.

Theorem 3.2: Owing to $\hat{x}_2 \neq 0$, the vector \hat{x}_2 can't reach a constant value in the dynamic process. In this case, the convergence conditions for the estimator are:

- (1) The base vector $\hat{x}_1(k/k-1)$ is convergent;
- (2) The values of $\hat{x}_{2_{\max}}$ and $\hat{x}_{2_{\min}}$ are bounded. It can be expressed as:

$$\begin{cases} \hat{x}_{2_{\min}} \geq Q \\ \hat{x}_{2_{\max}} \leq P \end{cases} \quad (27)$$

Where $P \in \mathbb{R}$ and $Q \in \mathbb{R}$.

Proof 3.2: Based on the **proof 3.1**, we can know that the base vector of \hat{x}_1 is convergent. So it just needs to prove the value of $\hat{x}_{2_{\max}}$ and $\hat{x}_{2_{\min}}$ are bounded. According to (20), it is obvious that for any $k \in [1, \infty)$, there must be $g_1(k) \in [g_{1_{\min}}, g_{1_{\max}}]$; and for any $k \in [1, \infty)$, there must be $f_1(k) \in [f_{1_{\min}}, f_{1_{\max}}]$. Then for any $k \in [1, \infty)$, it can obtain the following relationship:

$$\hat{x}_{2_{\min}} = \hat{x}_2(i/i-1) = \frac{g_1(i)\hat{x}_2(i-1/i-2) + (f_1(i) - f_1(i+1))}{g_1(i+1)} \quad (28)$$

$$\hat{x}_{2_{\max}} = \hat{x}_2(j/j-1) = \frac{g_1(j)\hat{x}_2(j-1/j-2) + (f_1(j) - f_1(j+1))}{g_1(j+1)} \quad (29)$$

In equation (20), T_e, v and \dot{v} are bounded variables, so g_1 and f_1 are bounded functions. With this in mind, it is obvious that $\hat{x}_{2_{\min}}$ and $\hat{x}_{2_{\max}}$ are bounded. Namely, the equation (26) is bounded. From the above analysis, it can be concluded that the BVCIE is convergent.

IV. EXPERIMENTAL RESULTS AND ANALYSIS

This section presents the practical implementation of the proposed BVCIE. It first describes briefly the tested EMHT and the travelling condition. Then, the estimation performance is validated with heavy loads under bumpy road conditions, heavy loads under uphill road conditions, and no-load under bumpy road conditions. Moreover, the performance of the proposed estimator is compared with other methods. Finally the sensitivity of the estimation results by the parameters of drag coefficient, the effective rolling friction coefficient, and the wheel radius are analyzed.

A. Experimental EMTH and Travelling Condition

To validate the performance of the proposed estimator, the EMHT used for this experiment is a 930E, produced by Komatsu, is one of the most commonly used EMHTs. The basic design parameters are shown in Table I. It is equipped with wheel rotational speed sensors and different traction motor sensors to obtain the vehicle velocity v and traction motor torque T_e . The tested 930E is working at the mining site of a mine company located at Haerwusu, Inner Mongolia, China. The route line information is collected by a high-precision GPS device. This high-precision GPS device consists of multiple satellites, fixed base stations and mobile base stations.

Moreover, the technologies of multipoint location and differential positioning are used. The measured information includes the coordinate and the altitude, and the route line can be shown in Fig. 5. With the information of route line and altitude, it can easily calculate the relative height by selecting the starting point as the reference point. The travel cycle of 930E includes loading, hauling, dumping and returning. The conditions for the heavy loads transport consist of a bumpy road and an uphill road owing to the EMHT working in the open-pit mine. In every travelling cycle, the 930E first travels with heavy loads under bumpy road conditions in a long distance of about 3.7 km, then travels with heavy loads under an uphill road condition within a short distance about 0.9 km. After finishing these two road sections, the 930E arrived at the dumping point. At the dumping point, the 930E needed about one minute for dumping, and after the dumping finished, the 930E went back following the same route line. As the brake needs to be applied during the back route line of the downhill, the experimental tests were only done on three cases. Case I is the condition of a normal cruise road condition for heavy loads; case II is the condition of an uphill road for heavy loads; and case III is the condition for no-loads. Before these tests, the total mass of 930E was measured by the truck weighing system in advance and the road grade was calculated by the relative height of the mine road.

TABLE I
DESIGN PARAMETERS AND SPECIFICATION OF 930E

Name	Symbol	Values	Unit
Vehicle mass	M_0	210187	kg
Air density	ρ	1.2258	N s ² /m ⁴
Wheel radius	r	1.6	m
Maximum total mass	M_{max}	501974	kg
Vehicle front area	A	64.0435	m ²
Maximum velocity	V_{max}	64.5	km/h
Identified drag coefficient	\hat{C}_d	0.45	-
Identified effective rolling friction coefficient	$\hat{\mu}$	0.2	-



Fig. 5. Process flow diagram for EMHT in the mining operation.

B. Estimation Results of Case I

In the bumpy road condition, the travel route line has no large slope but many bumps due to the extensive unpaved road network at the open-pit mine. This test selected a general bumpy road with about 3600 meters in distance, and approximately $M=460000$ kilograms in total mass. The relative height of this road is obtained by GPS, which is shown in Fig. 6(a). The relative height information demonstrates the time-varying nature of the mine road conditions. From the road's relative height information, it can be known that the

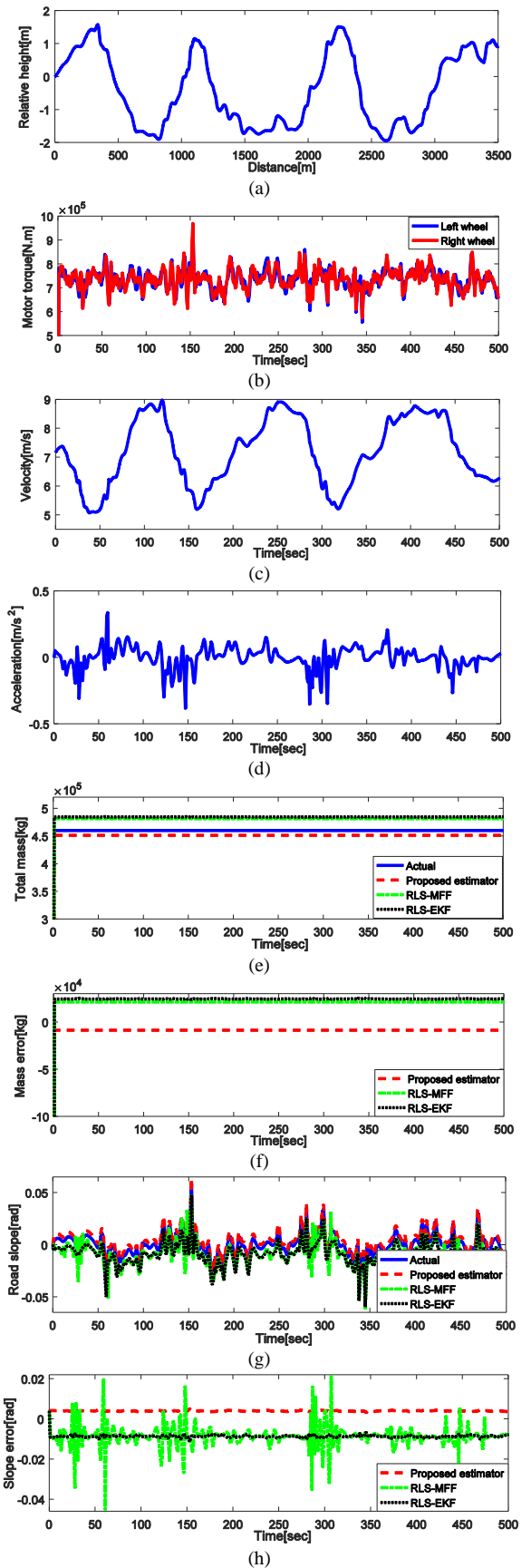


Fig. 6. Estimation results of heavy loads in bumpy road conditions. (a) Road's relative height. (b) Motor torques. (c) Vehicle speed. (d) Vehicle acceleration. (e) Vehicle total mass. (f) Mass error. (g) Road slope. (h) Road's slope error.

road's relative height varies between -2 to 2 meters. In the bumpy road condition, the measurement motor torque and the vehicle velocity are shown in Fig. 6(b) and Fig. 6(c). With the EMHT's velocity in Fig. 6(c), it is easy to calculate the acceleration, and the result is shown in Fig. 6(d). In the whole test process, the brake is disabled. The results in Fig. 6(e), Fig. 6(f), Fig. 6(g) and Fig. 6(h) show the performances of BVCIE for the estimation of the vehicle's total mass and the road grade. From Fig. 6(e), it is clear that the convergence of total vehicle mass by RLS with multiple forgetting factors (RLS-MFF), hybrid algorithm combining RLS and EKF (RLS-EKF) and the proposed estimator in this paper are all fast. However, the method in this paper provides a mass estimation \hat{M} that is closer to the actual vehicle mass. Moreover, The Fig. 6(f) reflects the error of the vehicle's total mass. It can be seen that the error is close to zero by the proposed estimator in this paper. The Fig. 6(g) reflects the result of the estimated road grade, and it can be known that the estimated $\hat{\theta}$ is closer to the actual road condition by our proposed estimator. The Fig. 6(h) reflects the results of the road grade error. Though there exist errors between the actual road grade and the estimated road grade by different methods, there exist fewest errors by the estimator in this paper. In order to compare the proposed estimator performance with RLS-MFF and RLS-EKF in detail, the index of root-mean-squared (RMS) error is used, and the comparative results are shown in Table II. According to the RMS results in TABLE II, it can be easily known that the proposed estimator in this paper has a better performance.

TABLE II

TOTAL MASS AND ROAD GRADE RMS ERRORS OF DIFFERENT ESTIMATORS FOR CASE I

Name	Proposed estimator	RLS-MFF	RLS-EKF
Total mass	2.2277×10^4	2.9632×10^4	3.2018×10^4
Road grade	0.004	0.0103	0.0087

C. Estimation Results of Case II

In the uphill condition with heavy loads, the travel road is with a large slope. The EMHT traveling on the uphill road with heavy loads is an important case in the mineral transporting process. Owing to the great total mass of 930E, the reliability control in the uphill road condition is a difficult problem. To improve the control performance in the uphill road with heavy loads, it requires the estimation of vehicle parameters and the road condition, such as the total mass and the road grade accuracy. For this reason, we tested the proposed estimator in the uphill road condition with heavy loads. The test road is in the same travelling cycle with IV (B). The tested uphill road is about 920 meters long, and the total mass is the same as in IV (B), approximately $M=460000$ kilograms. The relative height of this road is shown in Fig. 7(a). It can be seen that the height between the dumping point and the loading point is about 70 meters. In the uphill road condition with heavy loads, the measurement motor torque and the vehicle speed are shown in Fig. 7(b) and Fig. 7(c), and the EMHT's acceleration is shown in Fig. 7(d). For the measurement of the motor torque and the vehicle velocity, the total mass of 930E and the road grade can be estimated with our proposed estimator. The estimation results are shown in Fig. 7(e) and Fig. 7(g). The Fig. 7(e) shows that the total mass estimation is better than that with the methods of RLS-MFF and RLS-EKF. According to the

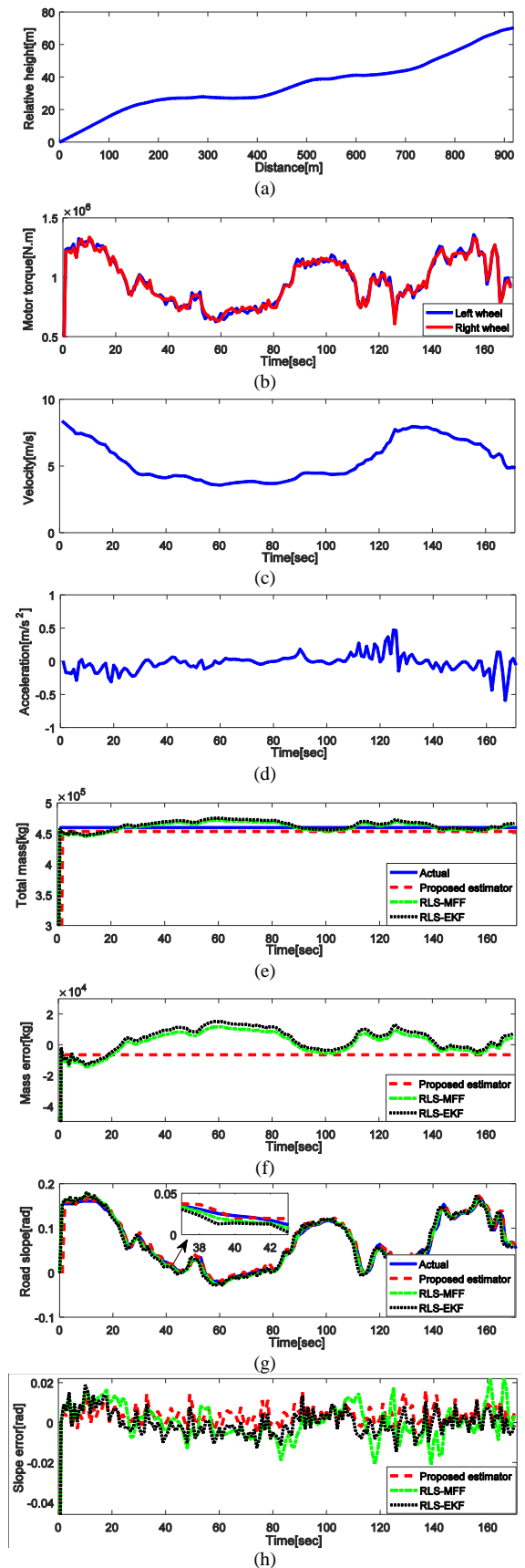


Fig. 7. Estimation results with heavy loads in the uphill road condition. (a) Road's relative height. (b) Motor torques. (c) Vehicle speed. (d) Vehicle acceleration. (e) Vehicle total mass. (f) Mass error. (g) Road slope. (h) Road's slope error.

zooming-in curves in Fig. 7(g), the estimated road grade with the proposed estimator is closer to the real value. The total mass error and the road grade error are shown in Fig. 7(f) and Fig. 7(h), respectively. From them we can know that the estimator's performance is still good. Furthermore, the RMS results of this test are shown in TABLE III. The results show that the proposed estimator is better than RLS-MFF and RLS-EKF.

TABLE III
TOTAL MASS AND ROAD GRADE RMS ERRORS OF DIFFERENT ESTIMATORS FOR CASE II

Name	Proposed estimator	RLS-MFF	RLS-EKF
Total mass	3.5760×10^4	3.5859×10^4	3.6127×10^4
Road grade	0.0133	0.0146	0.0134

D. Estimation Results of Case III

In the mineral transporting process, the returning with no-load is also an important part. In order to verify the proposed estimator performance in different load conditions, the returning with no-load in the bumpy road condition is also tested. This test selected the same bumpy road with IV(B). After the 930E finished dumping, we weighed the 930E again, and the total mass is approximately $M=210400$ kilograms, almost the same with the prior measurement. The relative height of this road is shown in Fig. 8(a), which is the reverse road condition in Fig. 6(a). In the bumpy road condition with no-load, the 930E velocity is faster than the process with heavy loads. By the vehicle sensors, the motor torque and the vehicle speed are measured and shown in Fig. 8(b) and Fig. 8(c), and the acceleration is shown in Fig. 8(d). Similar to the hauling process, in the whole test process, the brake is disabled. The results in Fig. 8(e) and Fig. 8(g) show the good performance of the BVCIE for the estimation of the total vehicle mass and the road grade, respectively. From the results in Fig. 8(f) and Fig. 8(h), it is clear that the estimator proposed in this paper provides a simultaneous estimation of the vehicle's total mass \hat{M} and the road grade $\hat{\theta}$ with good accuracy. Moreover, the RMS results in TABLE IV indicate that the proposed estimator in this paper has a better performance compared with RLS-MFF and RLS-EKF.

TABLE IV
TOTAL MASS AND ROAD GRADE RMS ERRORS OF DIFFERENT ESTIMATORS FOR CASE III

Name	Proposed estimator	RLS-MFF	RLS-EKF
Total mass	1.2304×10^4	1.3016×10^4	1.3707×10^4
Road grade	0.0045	0.0059	0.0054

E. Sensitivity Analysis

The above experiments are tested with the estimation parameters $\hat{\mu}=0.2$, $\hat{c}_d=0.45$. For the experiments in IV (B), IV (C) and IV (D), we assumed that the estimated parameters meet our needs. In order to analyze how much the mass and road grade estimation results are sensitive to these parameters, we changed the drag coefficient and the effective rolling friction coefficient once at a time and observed the performance of the estimation results. In this estimation, the RMS error is used to reflect the sensitivity of the estimation. We performed the analysis with the experimental set of data used in section IV (B), and the results are shown in Fig. 9 and Fig. 10. According to literature [46], in a realistic range, a 50% variation of the coefficient of effective rolling resistance caused, in the worst

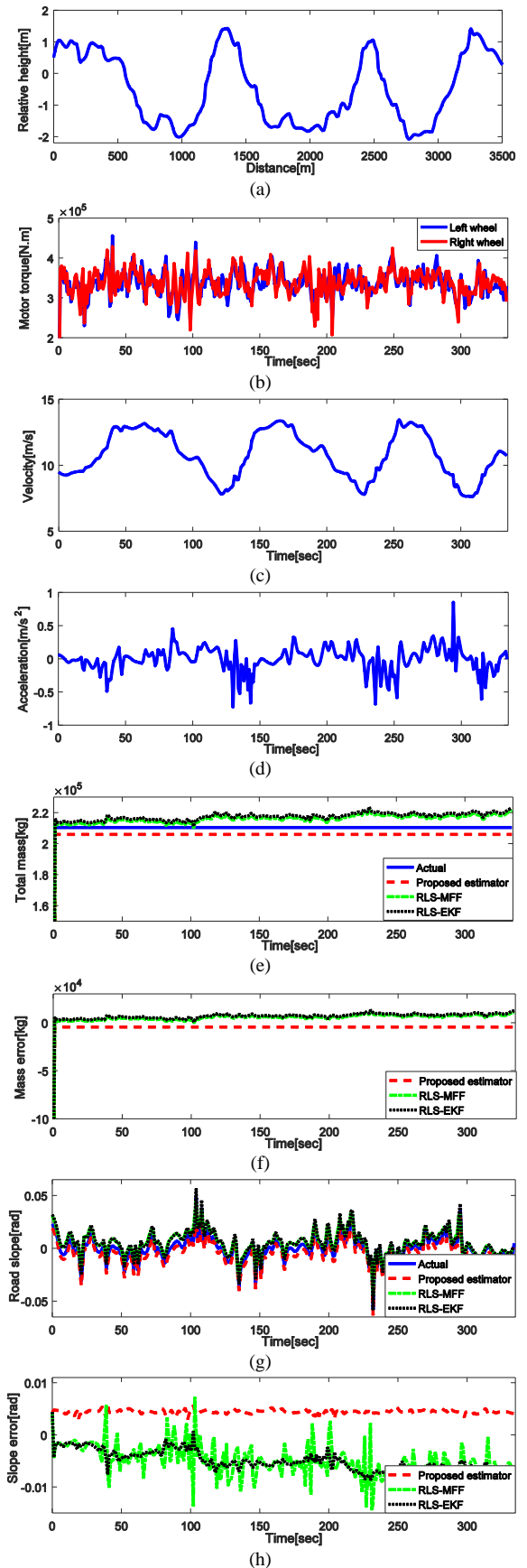


Fig. 8. Estimation results with no-load in a bumpy road condition. (a) Road's relative height. (b) Motor torques. (c) Vehicle speed. (d) Vehicle acceleration. (e) Vehicle total mass. (f) Mass error. (g) Road slope. (h) Road's slope error.

case, less than 25% change in the RMS error of grade estimations. According to Fig. 9, it can be known that a 50% change in drag coefficient within a feasible range caused less than 25% change of error in the grade and the mass estimations. Similarly, from Fig. 10, it can be known that a 50% change in effective rolling friction coefficient within a feasible range caused less than 25% change of error in the grade and mass estimations.

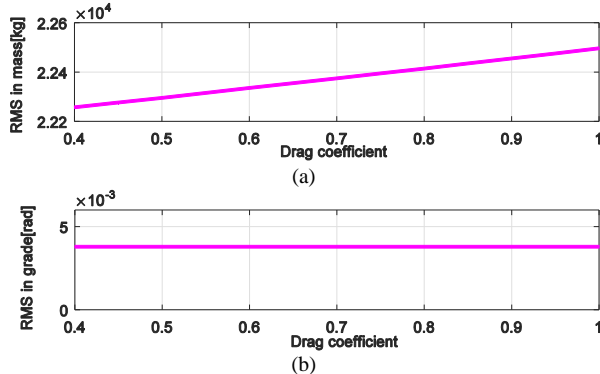


Fig. 9. Sensitivity of the estimation with respect to drag coefficient ($\mu=0.2$). (a) RMS in mass. (b) RMS in road grade.

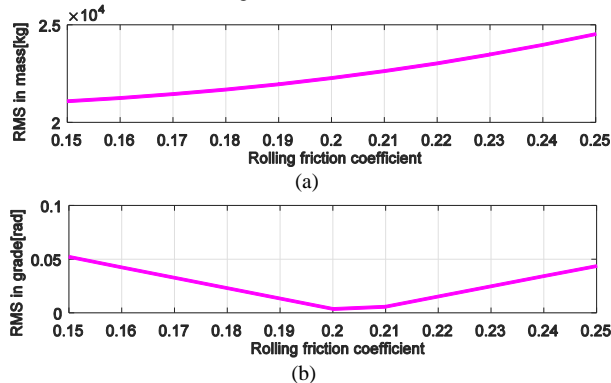


Fig. 10. Sensitivity of the estimation with respect to effective rolling friction coefficient ($C_r=0.45$). (a) RMS in mass. (b) RMS in road grade.

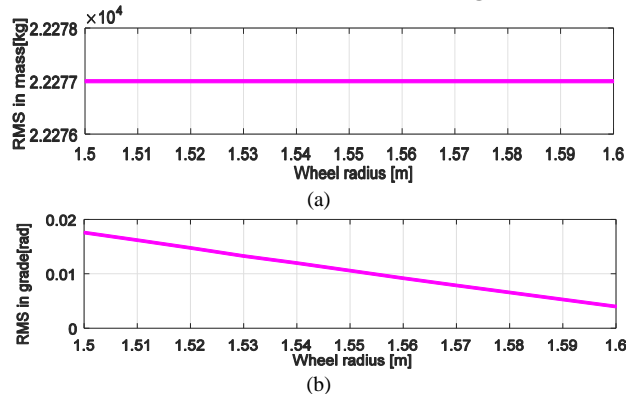


Fig. 11. Sensitivity of the estimation with respect to wheel radius ($\mu=0.2$, $C_r=0.45$). (a) RMS in mass. (b) RMS in road grade.

Moreover, for the experiments in IV (B), IV (C) and IV (D), we treat the wheel radius as a constant and it can be obtained accurately. However, in reality, the wheel radius may vary in the running process, which will affect the estimation results. In order to see how much the variation of wheel radius affects the estimation results, we changed the wheel radius once at a time and observed the performance of the estimation results. As shown in Fig. 11, it can be known that the RMS in total mass is nearly not affected by the variation of wheel radius. The RMS

in road grade presents slight fluctuation due to the variation of wheel radius. However, compared with the RMS results in IV (B), IV (C) and IV (D), the fluctuations of RMS in road grade are in confidence interval.

V. CONCLUSION

In this paper, a novel on-line simultaneous estimation of vehicle mass and road grade method is proposed and applied in 930E. The estimator is first designed through selecting a constant which is estimated as a base vector. It then uses cross iteration strategy to update the older information. Moreover, the estimator has been proved to be converged. The estimation results using 930E have validated the proposed estimator with good performances. Though there are some errors in the mass and the road grade, the estimation results show good accuracy on the whole. The vehicle mass and the road grade of 930E estimated by BVCIE proposed in this paper can be utilized in 930E's traction system controller and its safety system controller design, and it will significantly improve the control performance. Moreover, the proposed estimator can be utilized for other vehicle mass and road grade estimations, which is important for the intelligent control technology in autonomous vehicles. Based on the research results in this paper, the more advanced vehicle control method for EMHT is the authors' next research focus.

REFERENCES

- [1] Z. Allahkarami, A. R. Sayadi, and A. Lanke, "Reliability Analysis of Motor System of Dump Truck for Maintenance Management," *Springer International Publishing*, pp.681-688, 2016.
- [2] E. J. Ruth, "Automated pantograph control for mining truck power system," *ed: WO*, pp.1-15, 2014.
- [3] R. Ekyalimpa, S. M. Abourizk, and R. Wales, "A Special Purpose Simulation Template for Modeling Tire Usage of Mining Truck Fleet," *Construction Research Congress*, pp. 1074-1083, 2012.
- [4] W. G. Koellner, G. M. Brown, J. Rodriguez, and J. Pontt, "Recent advances in mining haul trucks," *IEEE Trans. Ind. Electron.*, vol. 51, pp. 321-329, 2004.
- [5] W. Wei and X. Zhang, "Research of Active Disturbances Rejection Control in Electric Wheel Dump Truck Speed Regulation System," *Mineral Engineering Research*, vol. 138, pp. 1945-1952, 2010.
- [6] A. Saadatmand and J. Sattarvand, "Application of ARENA Simulation Software for Evaluation of Open Pit Mining Transportation Systems – A Case Study," *Iscsm*, pp. 213-224, 2014.
- [7] D. K. Ahangaran, A. B. Yasrebi, A. Wetherelt, and P. Foster, "Real-time dispatching modelling for trucks with different capacities in open pit mines," *Instytut Mechaniki Górotworu Pan*, vol.57, pp. 39-52, 2012.
- [8] Chaowasakoo, Patarawan, et al. "Digitalization of mine operations: Scenarios to benefit in real-time truck dispatching," *International Journal of Mining Science and Technology* 27.2, pp. 229-236, 2017.
- [9] A. A. Bazzazi, M. Osanloo, and B. Karimi, "A new fuzzy multi criteria decision making model for open pit mines equipment selection," *Asia-Pacific Journal of Operational Research*, vol. 28, pp.279-300, 2011.
- [10] P. Bodziony, Z. Kasztelewicz, and P. Sawicki, "The Problem of Multiple Criteria Selection of the Surface Mining Haul Trucks," *Archives of Mining Sciences*, vol. 61, 2016.
- [11] Y. J. Zhang, J. Zhang, and X. K. Chen, "A DSP-Based Transmission Control System of 154t Electrical Wheels Autonomous Dump Truck," in *Eighth International Conference on Electrical Machines and Systems*, pp. 1650-1654, 2005.
- [12] Z. Liu, R. Wan, Y. Shi, and H. Chen, "Simulation Analysis of Traction Control System for Four-Wheel-Drive Vehicle Using Fuzzy-PID Control Method," *Communications in Computer & Information Science*, vol. 201, pp. 250-257, 2011.
- [13] J. Wang, Y. Zhang, J. Zhang, C. Luo, J. Wang, Y. Zhang, *et al.*, "Study of Control Strategies for Transmission system of Electrical Wheels

- Autonomous Dump Truck," in *Proceedings of the 11-(th) International Conference on Electrical Machines and Systems Volume 4*, pp. 2192-2195, 2008.
- [14] H. Sadjadian, S. Ozgoli, and M. Jalalifar, "Design and implementation of automatic transmission electronic control system for mining trucks," *International Conference on System Science, Engineering Design and Manufacturing Informatization*, pp. 1-4, 2011.
 - [15] K. Dewi, "Design and simulation of control in electrical slip based on wheel electrical haul truck traction control using fuzzy adaptive," *Master Thesis of Electrical Engineering*, 2011.
 - [16] A. M. Morad, M. Pourgol-Mohammad, and J. Sattarvand, "Application of reliability-centered maintenance for productivity improvement of open pit mining equipment: Case study of Sungun Copper Mine," *Journal of Central South University*, vol. 21, pp. 2372-2382, 2014.
 - [17] A. Soofastaei, S. M. Aminossadati, M. S. Kizil, and P. Knights, "A discrete-event model to simulate the effect of truck bunching due to payload variance on cycle time, hauled mine materials and fuel consumption," *International Journal of Mining Science and Technology*, vol. 26, pp. 745-752, 2016.
 - [18] Vries, Jelle De, et al. "Determinants of safe and productive truck driving: Empirical evidence from long-haul cargo transport." *Transportation Research Part E Logistics & Transportation Review* 97, pp.113-131, 2017.
 - [19] SHENYan-hua, XU Min, JIN Chun, et al. "Operator health risk evaluation of off-highway dump truck under shovel loading condition," *Journal of Central South University*, vol. 22, pp. 2655-2664, 2015.
 - [20] R. R. Obaid and R. H. Ahmad, "Automatic Guidance System for Trolley-Powered Mining Haul Trucks," *Industry Applications Society Meeting, 2009. Ias*, pp. 1-6, 2009.
 - [21] M. Azizi and E. Tarshizi, "Autonomous control and navigation of a lab-scale underground mining haul truck using LiDAR sensor and triangulation - feasibility study," *Industry Applications Society Meeting*, pp. 1-6, 2016.
 - [22] A. Soofastaei, S. M. Aminossadati, M. S. Kizil, and P. Knights, "A comprehensive investigation of loading variance influence on fuel consumption and gas emissions in mine haulage operation," *International Journal of Mining Science and Technology*, vol. 26, pp. 995-1001, 2016.
 - [23] Soofastaei, Aminossadati, Saiedi, Arefi, Mohammad, Kizil, et al., "Development of a multi-layer perceptron artificial neural network model to determine haul trucks energy consumption," *International Journal of Mining Science and Technology*, vol. 26, pp. 285-293, 2016.
 - [24] A. Soofastaei, S. Aminossadati, P. Knights, and M. Kizil, "Reducing Fuel Consumption of Haul Trucks in Surface Mines Using Artificial Intelligence Models," *Coal Operators' Conference*, 2016.
 - [25] S. Mirzaei and A. Fernandez, "Retard system solution on electric mining trucks," *Sensorless Control for Electrical Drives*, pp. 1-5, 2013.
 - [26] Q. Zhang, L. Lapierre, and X. Xiang, "Distributed Control of Coordinated Path Tracking for Networked Nonholonomic Mobile Vehicles," *IEEE Trans. Ind. Inf.*, vol. 9, pp. 472-484, 2012.
 - [27] Y. W. Liang, C. C. Chen, D. C. Liaw, and Y. T. Wei, "Nonlinear Reliable Control With Application to a Vehicle Antilock Brake System," *IEEE Trans. Ind. Inf.*, vol. 9, pp. 2114-2123, 2013.
 - [28] Y. Chen, X. Li, C. Wiet, and J. Wang, "Energy Management and Driving Strategy for In-Wheel Motor Electric Ground Vehicles With Terrain Profile Preview," *IEEE Trans. Ind. Inf.*, vol. 10, pp. 1938-1947, 2014.
 - [29] R. Wragge-Morley, G. Herrmann, P. Barber, and S. Burgess, "Information fusion for vehicular systems parameter estimation using an extended regressor in a finite time estimation algorithm," *Ukacc International Conference on Control*, pp. 401-406, 2014.
 - [30] Kim, Seungki, et al. "Development of algorithms for commercial vehicle mass and road grade estimation." *International Journal of Automotive Technology* 18.6 pp.1077-1083, 2017.
 - [31] Y. Sebsadji, S. Glaser, S. Mammar, and J. Dakhilallah, "Road slope and vehicle dynamics estimation," *American Control Conference*, pp. 4603-4608, 2008.
 - [32] Jauch, Jens, et al. "Road Grade Estimation with Vehicle Based Inertial Measurement Unit and Orientation Filter." *IEEE Sensors Journal* 99 pp.1-9, 2017.
 - [33] Altmannshofer, Simon, and C. Endisch. "Robust vehicle mass and driving resistance estimation." *American Control Conference IEEE*, pp. 6869-6874, 2016.
 - [34] Brown, Alexander A., and S. N. Brennan. "Model-Based Vehicle State Estimation Using Previewed Road Geometry and Noisy Sensors." *ASME 2012, Dynamic Systems and Control Conference Joint with the Jsme 2012, Motion and Vibration Conference*, pp.591-600, 2012.
 - [35] Jo, Kichun, M. Lee, and M. Sunwoo. "Road Slope Aided Vehicle Position Estimation System Based on Sensor Fusion of GPS and Automotive Onboard Sensors." *IEEE Transactions on Intelligent Transportation Systems* 17.1, pp.250-263, 2015.
 - [36] S. Dan and D. L. Simon, "Constrained Kalman filtering via density function truncation for turbofan engine health estimation," *International Journal of Systems Science*, vol. 41, pp. 159-171, 2010.
 - [37] J. Davins-Valldaura, F. Plestan, S. Moussaoui, and G. Pita-Gil, "Design and Optimization of Nonlinear Observers for Road Curvature and State Estimation in Automated Vehicles," *IEEE Trans. Intell. Transp. Syst.*, vol. (99), pp. 1-13, 2017.
 - [38] L. Hammarstrand, M. Fatemi, Á. F. García-Fernández, and L. Svensson, "Long-Range Road Geometry Estimation Using Moving Vehicles and Roadside Observations," *IEEE Trans. Intell. Transp. Syst.*, vol. 17, pp. 2144-2158, 2016.
 - [39] M. N. Mahyuddin, J. Na, G. Herrmann, X. Ren, and P. Barber, "Adaptive Observer-Based Parameter Estimation With Application to Road Gradient and Vehicle Mass Estimation," *IEEE Trans. Ind. Electron.*, vol. 61, pp. 2851-2863, 2013.
 - [40] B. Li, J. Zhang, H. Du, and W. Li, "Two-layer structure based adaptive estimation for vehicle mass and road slope under longitudinal motion," *Measurement*, vol. 95, pp. 439-455, 2017.
 - [41] M. L. McIntyre, T. J. Ghotikar, A. Vahidi, X. Song, and D. M. Dawson, "A Two-Stage Lyapunov-Based Estimator for Estimation of Vehicle Mass and Road Grade," *IEEE Trans. Veh. Technol.*, vol. 58, pp. 3177-3185, 2009.
 - [42] V. Winstead and I. V. Kolmanovsky, "Estimation of road grade and vehicle mass via model predictive control," *IEEE Conference on Control Applications*, pp. 1588-1593, 2005.
 - [43] B. L. Boada, D. Garcia-Pozuelo, M. J. L. Boada, and V. Diaz, "A Constrained Dual Kalman Filter Based on pdf Truncation for Estimation of Vehicle Parameters and Road Bank Angle: Analysis and Experimental Validation," *IEEE Trans. Intell. Transp. Syst.*, vol.99, pp. 1-11, 2017.
 - [44] Liu X Y, Alfi S, Bruni S. "An efficient recursive least square-based condition monitoring approach for a rail vehicle suspension system". *Vehicle System Dynamics*, 54(6), pp.814-830, 2016.
 - [45] Han, Weixin, Z. Wang, and Y. Shen. "Fault estimation for a quadrotor unmanned aerial vehicle by integrating the parity space approach with recursive least squares." *Proceedings of the Institution of Mechanical Engineers Part G Journal of Aerospace Engineering* 1 09544100 1769179, 2017.
 - [46] A. Stefanopoulou, "Recursive least squares with forgetting for online estimation of vehicle mass and road grade: theory and experiments," *Vehicle System Dynamics*, vol. 43, pp.31-55, 2005.
 - [47] A. Vahidi, A. Stefanopoulou, and H. Peng, "Experiments for Online Estimation of Heavy Vehicle's Mass and Time-Varying Road Grade," *Dynamic Systems and Control*, pp. 451-458, 2003.
 - [48] Z. Yu, Y. Feng, L. Xiong, and X. Wu, "Vehicle Mass Estimation for Four In-Wheel-Motor Drive Vehicle," *Electrical Engineering and Control. Springer Berlin Heidelberg*, vol.98, pp. 117-125, 2011.
 - [49] Y. Sun, L. Li, B. Yan, C. Yang, and G. Tang, "A hybrid algorithm combining EKF and RLS in synchronous estimation of road grade and vehicle 'mass for a hybrid electric bus," *Mechanical Systems & Signal Processing*, vol. s 68-69, pp. 416-430, 2016.
 - [50] Raffone, Enrico. "Road slope and vehicle mass estimation for light commercial vehicle using linear Kalman filter and RLS with forgetting factor integrated approach." *International Conference on Information Fusion IEEE*, pp.1167-1172, 2013.
 - [51] S. Dasgupta, Y. Shrivastava, and G. Krenzer, "Persistent excitation in bilinear systems," *IEEE Trans. Autom. Control*, vol. 36, pp. 305-313, 1991.



Ying Zhang(S'16) received the B.E degree in engineering from Henan University of Technology, in 2014, and the M.E degree in engineering from Hunan University, Hunan, in 2016. He is currently pursuing the Ph.D degree in Computer Science and Technology at Hunan University. His current research interests include Modeling, Estimation and Control of intelligent vehicles. He is a member of the IEEE, and the IEEE Vehicular Technology Society. He is a reviewer of IEEE.



Yingjie Zhang received the Ph.D. degree from Hunan University of Control Theory and Control Engineering, Hunan, in 2005. He was an UIO visiting scholar from 2010–2011 at Norway. He is the director of Institute of Industry Energy-saving Control & Evaluation, Hunan University. He is an associate professor at the College of Computer Science and Electric Engineering, Hunan University of Intelligent Control, China. His research interests include intelligent control, computational intelligence and Energy-optimized control. He has published more than 50 papers in refereed journals and conferences.



Yun Feng received the B.E degree in engineering from Henan University of Technology, in 2014, and the M.E degree in engineering from Hunan University, Hunan, in 2017. she is an engineer of the Company of Bozhon (Suzhou) Precision Industry Technology Co., Ltd, Jiangsu province, Suzhou. Her current research interests include Digital Image Processing, Computer vision, and intelligent control.



Zhaoyang Ai (M'14) received the Ph.D degree in Linguistics from Hunan University, Changsha, China. He is now working as associate professor with the Institute of Cognitive Control and Lingua-biophysics, CFL, Hunan University. He was visiting scholar at Yale University. He has published over 10 research papers in international journals and conferences in addition to three academic books. His research is focused on cognitive control and lingua-biophysics, and his research interests include intelligent translation and

interpretation, linguistics, cognitive superconductivity, informatics, smart control and efficiency studies. He is a member of the IEEE, the IEEE Council of Superconductivity, IEEE Communications Society, and IEEE Information Theory Society.



Zuolei Hu received the B.S. degree in electronic and information engineering from Nanyang Institute of Technology, China, in 2014, and the M.E degree in engineering from Hunan University, Hunan, in 2017. Currently, he is working toward the Ph.D degree in Computer Science and Technology at Hunan University. He current research interests include modeling of base station energy consumption system, electricity allocation of base station.